

ChemComm

Accepted Manuscript



This article can be cited before page numbers have been issued, to do this please use: M. Makrinich and A. Goldbourn, *Chem. Commun.*, 2019, DOI: 10.1039/C9CC01176E.



This is an Accepted Manuscript, which has been through the Royal Society of Chemistry peer review process and has been accepted for publication.

Accepted Manuscripts are published online shortly after acceptance, before technical editing, formatting and proof reading. Using this free service, authors can make their results available to the community, in citable form, before we publish the edited article. We will replace this Accepted Manuscript with the edited and formatted Advance Article as soon as it is available.

You can find more information about Accepted Manuscripts in the [author guidelines](#).

Please note that technical editing may introduce minor changes to the text and/or graphics, which may alter content. The journal's standard [Terms & Conditions](#) and the ethical guidelines, outlined in our [author and reviewer resource centre](#), still apply. In no event shall the Royal Society of Chemistry be held responsible for any errors or omissions in this Accepted Manuscript or any consequences arising from the use of any information it contains.

COMMUNICATION

 ^1H -detected quadrupolar spin-lattice relaxation measurements under magic-angle spinning solid-state NMRReceived 00th January 20xx,
Accepted 00th January 20xxMaria Makrinich,^a Amir Goldbourt^{a,*}

DOI: 10.1039/x0xx00000x

Proton detection and phase-modulated pulse saturation enables the measurement of spin-lattice relaxation times of "invisible" quadrupolar nuclei with extensively large quadrupolar couplings. For nitrogen-14, efficient cross-polarization is obtained with a long-duration preparation pulse. The experiment paves the way to the characterization of a large variety of materials containing halogens, metals and more.

Magic-angle spinning solid-state NMR (MAS ssNMR) can provide detailed structural information for a wide variety of systems, and is particularly useful for non-soluble, or non-crystalline materials¹. The acquisition of spin-lattice NMR relaxation times in the solid-state provides information on dynamics, structure and mobility^{2–4}. However, a notable majority of these measurements are conducted on nuclei possessing a spin one-half such as hydrogen or carbon. Nevertheless, most elements (close to 75%) in the periodic table have nuclei with spins larger than one-half, including nitrogen, oxygen, most halogens, and most metals. Hence, they possess a nuclear quadrupole moment and are subjected to the magnetic nuclear quadrupolar interaction. Relaxation time measurements of quadrupolar nuclei are useful for many applications, including the determination of jump-rates (for ^7Li and other ions) in battery materials^{5–7}, ion hopping in materials⁸, the characterization of electronic states⁹, elucidating dynamics in proteins¹⁰, and more.

Unlike ^7Li , ^2H and ^{133}Cs , which have a small quadrupole moment, most quadrupolar nuclei still pose severe challenges to their characterization by NMR techniques due to the large size of the quadrupolar interaction. Quadrupolar T_1 spin-lattice relaxation measurements under MAS conditions are especially compromised since they require uniform excitation of the entire quadrupolar spin spectral manifold¹¹ in order to avoid the effects of spin-exchange processes, which lead to shorter recovery times, multi-exponential recovery curves even when they would have been mono-exponential otherwise, and failure to determine the actual relaxation rate. These effects have been nicely laid out by Yesinowski^{11,12}, who proposed a

non-synchronous train of pulses to efficiently saturate both central and satellite transitions of a half-integer quadrupolar nucleus. We have recently proposed a phase-modulated (PM) pulse that can fully saturate very broad quadrupolar spectra¹³, enabling to obtain accurate relaxation times, and demonstrated T_1 measurements of ^{11}B spins in 4-methoxyphenylboronic acid (a spin-3/2 with a nuclear quadrupolar coupling constant $C_Q=3.1$ MHz, equalling a quadrupolar frequency ν_Q of 1.55 MHz)¹⁴. However, many systems of interest contain quadrupolar nuclei that possess extensively large quadrupolar couplings, making them practically undetectable by MAS ssNMR techniques (hence: "invisible", or "unreceptive"), and thus are preferentially studied by static wide-line solid-state NMR¹⁵. Common examples of such quadrupolar nuclei are the halogens bromine, chlorine and iodine, with quadrupolar coupling constants of $\sim 10^0$ – 10^2 MHz. The detection of ^{14}N is even more complicated since it is an integer spin-1 lacking a central transition (CT). A CT exists only in quadrupolar nuclei with half-integer spins, is broadened only by the second order quadrupolar interaction, and is therefore more easily excited and detected. Since ^{14}N is a highly abundant (99.6%) nucleus, and highly common in all biological systems, the ability to easily measure its relaxation times in different systems could become highly beneficial.

The difficulty to directly detect many quadrupolar spins can be overpowered by indirect detection via protons hence allowing the measurement of their T_1 relaxation times. Indirect proton detection has recently become increasingly common due to the availability of fast-spinning MAS probes^{16–20} providing high-resolution ^1H spectra, and indirect detection of quadrupolar nuclei has been demonstrated in various cases^{21–25}. In particular, the manuscript of Rossini and coworkers²¹ discusses the sensitivity of ^1H -detected quadrupolar spectra obtained by utilizing two different transfer mechanisms, dipolar hetero-nuclear multiple quantum correlation (D-HMQC²⁶) and dipolar refocused insensitive nuclei enhanced by polarization transfer (D-RINEPT^{27,28}). Moreover, using D-RINEPT for polarization transfer they measured relaxation times of ^{35}Cl ($\nu_Q = 0.95$ MHz), ^{71}Ga ($\nu_Q = 2.9$ MHz) and ^{27}Al ($\nu_Q \cong 0.4$ MHz) at a spinning speed of 50 kHz by using proton detection and the saturation method of Yesinowski¹¹.

^a School of Chemistry, Sackler Faculty of Exact Sciences, Tel Aviv University, Ramat Aviv 6997801, Tel Aviv, Israel.
* amirgo@tauex.tau.ac.il

COMMUNICATION

Journal Name

Here we aim to make relaxation time measurements applicable to a wide range of quadrupolar frequencies and spins. Thus, the quadrupolar nucleus should be saturated by the PM pulse. Thus far, the performance of the PM pulse with respect to relaxation of quadrupolar spins with extensively large couplings has not been tested, since we aim at such spins that cannot be directly detected, or that their detection is extremely difficult and lengthy. However, the performance of the PM pulse with respect to such nuclei has been examined²⁹ by performing distance measurements to bismuth-209 in bismuth acetate (a spin-9/2 with a nuclear quadrupolar coupling constant $C_Q=256$ MHz, or a frequency ν_Q of ~ 11 MHz), and to bromine-79 in Butyltriphenylphosphonium bromide ($C_Q=11.3$ MHz, $\nu_Q = 5.64$ MHz). In both cases, the analytical fit of the data pointed to excellent saturation.

The approach to obtain quadrupolar spin-lattice relaxation times via ^1H detection is presented in Fig. 1a. The quadrupolar S-nucleus is saturated by the PM pulse, followed by a recovery interval. Excitation of the quadrupolar spin is obtained by a pulse of duration τ_p (which is $\pi/2$ for half-integer quadrupolar spins, but different for ^{14}N , see below) and followed by polarization transfer to the highly-sensitive ^1H nucleus, which can be readily detected. Since protons are used only as a detection channel, achieving high resolution is not essential, and the experiment can be performed at any desired spinning speed, low (< 15 kHz) or high (> 40 kHz). When the spinning speed is high the PM pulse must be adjusted accordingly by its mere extension, and was shown theoretically to provide excellent saturation properties even at fast spinning speeds³⁰. Also, enough polarization must be transferred from the quadrupolar nucleus to ^1H . Polarization transfer methods to or from the quadrupolar spin can be obtained in various ways, such as a simple cross polarization (CP³¹), D-HMQC²⁶, D-RINEPT^{27,28}, PRESTO³², and RESPIRATION-CP^{33,34}, with sensitivity gains depending on experimental conditions. Recent studies have compared the performance of D-RINEPT with D-HMQC²¹ and with PRESTO³⁵.

In order to simplify our experimental approach, and to focus on relaxation time measurements, we utilized the basic Hartman-Hahn ramped-CP polarization transfer technique. Nonetheless, any polarization transfer could be used for this purpose and the transfer efficiency affects the final sensitivity of detection but should not affect the measured value of T_1 . This latter statement should be taken with care. The relaxation time depends on the orientation and thus in principle, every crystallite has a different T_1 relaxation time. Yet, as shown by Hodgkinson et al., spinning averages this effect generating a similar T_1 value for every crystallite³⁶.

In order to initially demonstrate the validity of indirect quadrupolar T_1 measurements, we compare in Fig. 1 the ^{23}Na T_1 relaxation times in di-sodium hydrogen phosphate dihydrate ($\text{Na}_2\text{HPO}_4 \cdot 2\text{H}_2\text{O}$) measured directly and indirectly. In the direct approach (Fig. 1b) ^{23}Na is saturated with a PM pulse and then directly detected, while in the indirect approach, ^{23}Na relaxation is followed by a CT excitation pulse and finally the ^1H signal is detected after CP (Fig. 1c). Both experiments were fitted to a mono-exponential saturation recovery

curve $I(t)/I_0 = m(1 - a \cdot \exp(-t/T_1))$. Here m accounts for the maximum normalized signal intensity at time t_{max} ($m=1$ corresponds to ideal full recovery with no experimental error), and $a=1$ indicates complete saturation.

The results of the two experiments, given explicitly in the figure caption, yielded a recovery rate of ~ 6.9 s, with the difference being within the error range. The hydrogen detected approach is therefore reliable and does not require fast MAS or high-resolution thus making the approach applicable to any spinning frequency. As mentioned previously, at fast spinning speeds both the length of the PM pulse and the transfer mechanism must be optimized. It is important to point out, that $\text{Na}_2\text{HPO}_4 \cdot 2\text{H}_2\text{O}$ has two inequivalent sodium sites, having quadrupolar coupling constants (C_Q) of 1.63 and 2.36 MHz³⁷, and the mono-exponential nature of the recovery implies that these two sites have similar recovery rates. Moreover, since ^{23}Na is a spin-3/2 nucleus, two recovery rates are generally expected for each site given that the saturation was uniform³⁸. Therefore, either the extreme narrowing condition (the product of the Larmor frequency and the motional correlation time of sodium is smaller than one) can be assumed making the two rates equal, or the two recovery rates of each individual site are similar for some other reason^{12,14,39,40}.

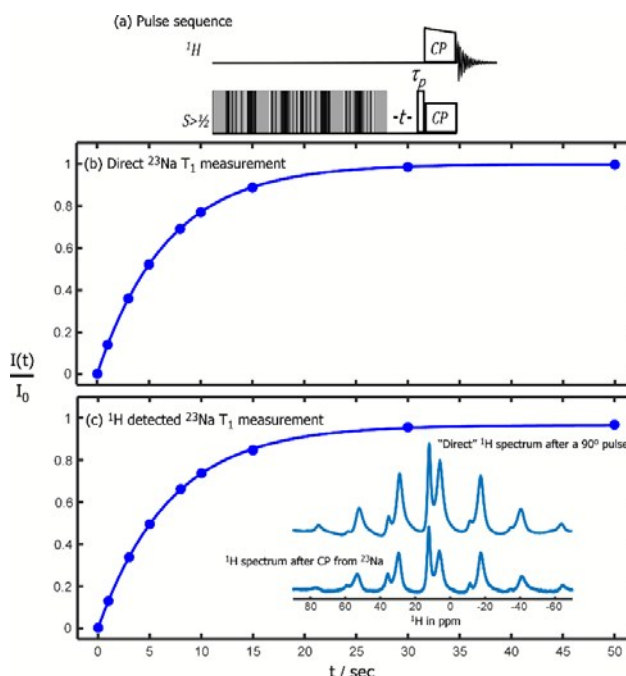


Fig. 1 ^{23}Na spin-lattice (T_1) relaxation measurements in di-sodium hydrogen phosphate dihydrate. (a) ^1H -detected Phase Modulated (PM) saturation recovery experiment. The phases in the PM pulse are color coded according to a white-black scale indicating 0–360°. The relative lengths of the pulse segments are preserved. Actual values have been reported before¹³. The phase cycle employs spin temperature inversion and is given in the SI. (b) Direct saturation recovery curve obtained at 45 °C. Here PM-saturation was followed by a variable delay t , selective central-transition excitation, and detection¹⁴. A mono-exponential fit to $I(t)/I_0 = m(1 - a \cdot \exp(-t/T_1))$ yields $m = 0.9983 \pm 0.0008$; $a = 0.9972 \pm 0.0019$; $T_1 = 6.79 \pm 0.03$ s. The fits were obtained with the 'cftool' in MATLAB and the errors report the 95% confidence. The error bars are smaller than the size of the marker. (c) ^1H -detected PM saturation recovery (45 °C) according to the sequence in (a) using a pulse length τ_p corresponding to a selective CT $\pi/2$ pulse. The

fit yields $m = 0.965 \pm 0.009$; $a = 1.00 \pm 0.02$; $T_1 = 7.0 \pm 0.4$ s. The inset shows a comparison between a Bloch-decay ^1H spectrum, obtained from a single 90° pulse excitation (top) and the ^1H spectrum after transferring the polarization from ^{23}Na (bottom, experimental time 17 min). More experimental details are available in the SI.

In order to further demonstrate the ability to apply the ^1H -detected PM-saturation recovery experiment to quadrupolar nuclei with extensively large couplings, even at this moderate spinning of 14 kHz, we chose to measure the relaxation times of ^{14}N (spin-1) in glycine and of ^{81}Br (spin-3/2) in Tetra-n-butylammonium bromide (TBAB). ^{14}N in glycine has a quadrupolar frequency of $\nu_Q \approx 1.77$ MHz⁴¹, and an attempt to directly detect ^{14}N in glycine would potentially require tens of thousands of scans⁴² and probably a very accurate setting of the magic angle. Our own attempts to measure ^{14}N did not produce any signal after one hour of signal collection. It is not practical therefore to measure its relaxation time directly. For TBAB, a quadrupolar coupling constant has not yet been reported, however similar compounds possess quadrupolar frequencies of 3–4 MHz ($C_Q \approx 6$ –8 MHz)⁴³ and our attempts to measure a ^{81}Br signal resulted in broad and distorted line shape (see SI). Thus for such spins, ^1H -detected measurements are the only way to obtain their relaxation rates, and accurate values can only be obtained if an efficient saturation scheme exists.

Fig. 2 shows the ^1H -detected recovery curves for ^{14}N and for ^{81}Br . Due to the large quadrupolar coupling constant of ^{14}N , the PM saturation pulse was extended to 50 rotor periods. This approach was demonstrated in a prior work²⁹ where we measured distances to bismuth-209 in bismuth acetate. For both spins we observed a good fit to a mono-exponential recovery curve. For a spin-1, a mono-exponential curve is expected under initial conditions of saturation regardless of the values of the single and double-quantum relaxation constants W_1 and W_2 , since although the two relaxation rates depend on W_1 and W_2 , the coefficient of one of them is zero⁴⁴. For a spin-3/2 a mono-exponential rate will be obtained under saturation only if $W_1=W_2$, which is a consequence of the fast motion regime, or an averaging effect of the spinning.

In order to generate ^{14}N polarization after the relaxation delay, its excitation pulse length must be optimized. Interestingly, we find that when the pulse length was 40–50 μs , an optimal signal was obtained using a radio-frequency (rf) power of $\nu_1=30$ kHz. This result differs from half-integer quadrupolar nuclei (such as ^{81}Br , Fig. 2b), for which a central-transition selective excitation is utilized. Another point to note is that clearly not all the glycine crystallites are uniformly excited during the pulse. Yet, whichever part of the spectrum that is excited, and transferred to ^1H , is reproducible in every time point measurement. It would therefore allow the measurement of reliable relaxation values. The result that a long excitation pulse maximizes the transfer efficiency to protons, implies that more than just single quantum ^{14}N coherences are excited and transferred to protons, as double-quantum transitions have a weaker nutation frequency⁴⁵ of the order ν_1^2/ν_Q . Since the type of excitation, transfer mechanism and excitation selectivity with respect to the crystallites is not clear at this stage, we have tested the measurement reliability by

obtaining T_1 curves for three different pulse lengths – a short pulse of 8.3 μs (equalling a $\pi/2$ pulse), an intermediate pulse of 25 μs , and a long pulse of duration 41 μs or 48 μs . Moreover, for the short and long pulses, we measured T_1 as a function of temperature in order to assess whether T_1 depends on the excitation characteristics. Temperature dependence also allows us to examine if the relaxation we obtain is in the fast motion limit. Since short and long excitation pulses result in a different distribution of crystallite excitations, the result that the dependence on temperature of the two T_1 measurement sets is equal, and that the actual T_1 values are equal (within the error range) suggests that indeed we are measuring a real T_1 despite the selectivity of the pulse and CP transfer.

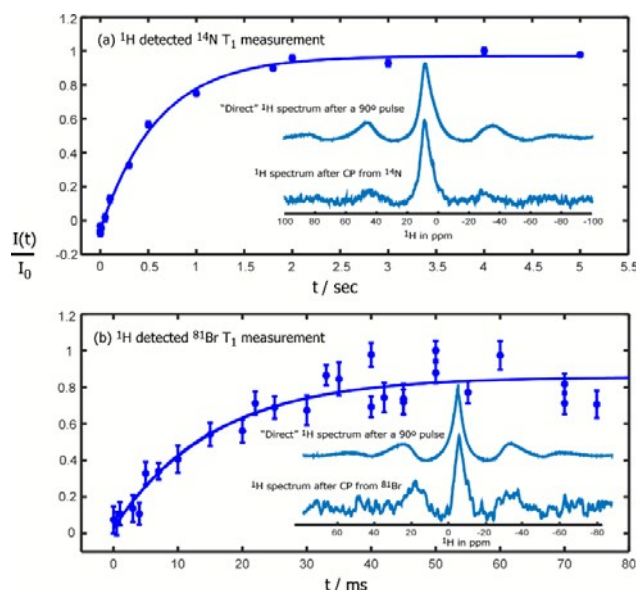
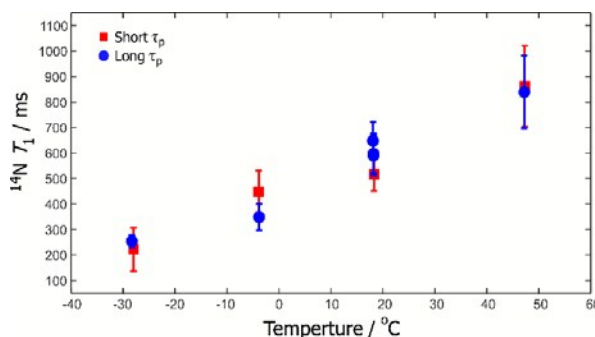


Fig. 2 (a) ^1H -detected ^{14}N PM-saturation recovery spin-lattice (T_1) relaxation measurement in natural-abundance glycine at 18 °C. The mono-exponential fit yields $m = 0.97 \pm 0.03$; $a = 1.06 \pm 0.03$; $T_1 = 598 \pm 77$ ms. The inset compares a Bloch decay spectrum (top) with a $\{^{14}\text{N}\}^1\text{H}$ CP spectrum (bottom). (b) ^1H -detected ^{81}Br PM-saturation recovery T_1 relaxation measurement in Tetra-n-butylammonium bromide (TBAB) at 45 °C. The fit to mono-exponential recovery yields $m = 0.86 \pm 0.07$; $a = 1.0 \pm 0.1$; $T_1 = 15 \pm 6$ ms. The inset compares a Bloch decay spectrum (top) with a $\{^{81}\text{Br}\}^1\text{H}$ CP spectrum (bottom, acquired in 10.7 min).

The temperature dependence of ^{14}N T_1 relaxation times appears in Fig. 3. We observe that T_1 increases with temperature and this implies that under the conditions in which we perform the experiment, the fast motion limit can be assumed.



COMMUNICATION

Journal Name

Fig. 3 Temperature dependence of ^{14}N T_1 relaxation times in glycine measured using a short excitation pulse of 8.3 μs (squares, red) and a long excitation pulse of 41 μs or 48 μs (circles, blue). Some points were measured more than once (18 $^\circ\text{C}$). The experimental saturation recovery curves and their fits can be found in the SI.

The T_1 relaxation time of ^{81}Br in TBAB, measured via proton detection, is shown in Fig. 2b. We obtained in this case a short recovery rate of 15 ± 6 ms. Here the detection sensitivity is low compared to ^{14}N and this is most probably the main cause for the larger error in the fit of the T_1 value (reported with a confidence level of 95%). We therefore attempted to measure the relaxation times of ^{81}Br directly. As shown in the SI, although the ^{81}Br spectrum was heavily distorted, we obtained a similar T_1 value as that of the indirect measurement. Also, both curves fit a mono-exponential decay, and since in the case of a spin-3/2 a mono-exponential fit is obtained only if $W_1=W_2$, it implies that the extreme narrowing condition might apply in this case as well.

In summary, combining a phase-modulated broad-banded quadrupolar-spin saturation pulse with ^1H -detection provides previously inaccessible relaxation rates of unresponsive quadrupolar spins with extensively large couplings, some of which cannot be directly detected using MAS. The method is applicable at any spinning rate since high resolution of the ^1H spectrum is not required, the length of the saturation pulse can be adjusted to perform optimally at a broad range of conditions, and the transfer can be achieved using various techniques such as CP as shown here, or other techniques such as D-RINEPT, D-HMQC and more. The experiment is therefore useful for the characterization of a large variety of ordered, disordered and porous materials.

This research was supported by the US-Israel binational science foundation, grant #2016169. We thank Dr. Uzi Eliav for fruitful discussions on ^{14}N excitation.

Conflicts of interest

There are no conflicts to declare.

Notes and references

1. T. Polenova, R. Gupta, and A. Goldbourt, *Anal. Chem.*, 2015, **87**, 5458–5469.
2. P. Schanda and M. Ernst, *Prog. Nucl. Magn. Reson. Spectrosc.*, 2016, **96**, 1–46.
3. T. Ueda, K. Kurokawa, Y. Kawamura, K. Miyakubo, and T. Eguchi, *J. Phys. Chem. C*, 2012, **116**, 1012–1019.
4. C. P. Jaroniec, *J. Magn. Reson.*, 2015, **253**, 50–59.
5. M. Wilkening and P. Heitjans, *Phys. Rev. B - Condens. Matter Mater. Phys.*, 2008, **77**, 1–13.
6. A. Kuhn, S. Narayanan, L. Spencer, G. Goward, V. Thangadurai, and M. Wilkening, *Phys. Rev. B - Condens. Matter Mater. Phys.*, 2011, **83**, 1–11.
7. C. P. Grey and N. Dupré, *Chem. Rev.*, 2004, **104**, 4493–4512.
8. R. E. Taylor, P. A. Beckmann, S. Bai, and C. Dybowski, *J. Phys. Chem. C*, 2014, **118**, 9143–9153.
9. S. H. Baek, B. J. Suh, E. Pavarini, F. Borsa, F. Borsa, R. G. Barnes, S. L. Bud'ko, and P. C. Canfield, *Phys. Rev. B - Condens. Matter Mater. Phys.*, 2002, **66**, 1045101–1045107.
10. X. Shi and C. M. Rienstra, *J. Am. Chem. Soc.*, 2016, **138**, 4105–4119.
11. J. P. Yesinowski, *J. Magn. Reson.*, 2015, **252**, 135–144.
12. J. P. Yesinowski, *J. Magn. Reson.*, 2006, **180**, 147–161.
13. E. Nimerovsky, R. Gupta, J. Yehl, M. Li, T. Polenova, and A. Goldbourt, *J. Magn. Reson.*, 2014, **244**, 107–13.
14. M. Makrinich, R. Gupta, T. Polenova, and A. Goldbourt, *Solid State Nucl. Magn. Reson.*, 2017.
15. R. W. Schurko, *Acc. Chem. Res.*, 2013, **46**, 1985–1995.
16. Y. Ishii, J. P. Yesinowski, and R. Tycko, *J. Am. Chem. Soc.*, 2001, **123**, 2921–2922.
17. E. K. Paulson, C. R. Morcombe, V. Gaponenko, B. Danchek, R. A. Byrd, and K. W. Zilm, *J. Am. Chem. Soc.*, 2003, **125**, 15831–6.
18. J. W. Wiench, C. E. Bronnimann, V. S. Y. Lin, and M. Pruski, *J. Am. Chem. Soc.*, 2007, **129**, 12076–12077.
19. D. H. Zhou and C. M. Rienstra, *Angew. Chemie - Int. Ed.*, 2008, **47**, 7328–7331.
20. G. P. Holland, B. R. Cherry, J. E. Jenkins, and J. L. Yarger, *J. Magn. Reson.*, 2010, **202**, 64–71.
21. A. Venkatesh, M. P. Hanrahan, and A. J. Rossini, *Solid State Nucl. Magn. Reson.*, 2017, **84**, 171–181.
22. S. Cavadini, A. Abraham, and G. Bodenhausen, *Chem. Phys. Lett.*, 2007, **445**, 1–5.
23. Y. Nishiyama, Y. Endo, T. Nemoto, H. Utsumi, K. Yamauchi, K. Hioka, and T. Asakura, *J. Magn. Reson.*, 2011, **208**, 44–48.
24. M. K. Pandey, H. Kato, Y. Ishii, and Y. Nishiyama, *Phys. Chem. Chem. Phys.*, 2016, **18**, 6209–6216.
25. M. Shen, J. Trébosc, O. Lafon, Z. Gan, F. Pourpoint, B. Hu, Q. Chen, and J. P. Amoureux, *Solid State Nucl. Magn. Reson.*, 2015, **72**, 104–117.
26. X. Lu, O. Lafon, J. Trébosc, G. Tricot, L. Delevoye, F. Méar, L. Montagne, and J. P. Amoureux, *J. Chem. Phys.*, 2012, **137**, 144201.
27. J. Trébosc, B. Hu, J. P. Amoureux, and Z. Gan, *J. Magn. Reson.*, 2007, **186**, 220–227.
28. C. Martineau, B. Bouchevreau, F. Taulelle, J. Trébosc, O. Lafon, and J. Paul Amoureux, *Phys. Chem. Chem. Phys.*, 2012.
29. M. Makrinich, E. Nimerovsky, and A. Goldbourt, *Solid State Nucl. Magn. Reson.*, 2018, **92**.
30. E. Nimerovsky, M. Makrinich, and A. Goldbourt, *J. Chem. Phys.*, 2017, **146**.
31. E. O. Stejskal, J. Schaefer, and J. S. Waugh, *J. Magn. Reson.*, 1977.
32. X. Zhao, W. Hoffbauer, J. Schmedt Auf Der Gönne, and M. H. Levitt, *Solid State Nucl. Magn. Reson.*, 2004, **26**, 57–64.
33. S. Jain, M. Bjerring, and N. C. Nielsen, *J. Phys. Chem. Lett.*, 2012, **3**, 703–708.
34. S. K. Jain, A. B. Nielsen, M. Hiller, L. Handel, M. Ernst, H. Oshkinat, Ü. Akbey, and N. C. Nielsen, *Phys. Chem. Chem. Phys.*, 2014, **16**, 2827.
35. R. Giovine, J. Trébosc, F. Pourpoint, O. Lafon, and J.-P. Amoureux, *J. Magn. Reson.*, 2019, **299**, 109–123.
36. D. C. Apperley, A. F. Markwell, I. Frantsuzov, A. J. Iltott, R. K. Harris, and P. Hodgkinson, *Phys. Chem. Chem. Phys.*, 2013, **15**, 6422–6430.
37. M. Edén and L. Frydman, *J. Phys. Chem. B*, 2003, **107**, 14598–14611.
38. E. R. Tunstall and D. P. Andrew, *Proc. Phys. Soc.*, 1961, **78**, 1.
39. P. S. Hubbard, *J. Chem. Phys.*, 1970, **53**, 985.
40. M. Witschas and H. Eckert, *J. Phys. Chem. A*, 1999, **103**, 10764–10775.
41. S. Cavadini, A. Lupulescu, S. Antonijevic, and G. Bodenhausen, *J. Am. Chem. Soc.*, 2006, **128**, 7706–7707.
42. T. Giavani, H. Bildsøe, J. Skibsted, and H. J. Jakobsen, *J. Magn. Reson.*, 2004, **166**, 262–272.
43. P. M. J. Szell and D. L. Bryce, in *Annual Reports on NMR Spectroscopy*, Elsevier Ltd., 1st edn., 2015, vol. 84, pp. 115–162.
44. A. Suter, M. Mali, J. Roos, and A. Brinkmann, *J. Phys. Condens. Matter*, 1998, **10**, 5977.
45. S. Vega, *J. Chem. Phys.*, 1978, **68**, 5518–5527.